Semi-Implicit Method for Three-Dimensional Compressible MHD Simulation

Douglas S. Harned*, W. Kerner

IPP 6/234 March 1984

MAX-PLANCK-INSTITUT FÜR PLASMAPHYSIK

8046 GARCHING BEI MÜNCHEN

MAX-PLANCK-INSTITUT FÜR PLASMAPHYSIK

GARCHING BEI MÜNCHEN

Semi-Implicit Method for Three-Dimensional Compressible MHD Simulation

Douglas S. Harned*, W. Kerner

IPP 6/234 March 1984

* Permanent address: Courant Institute of Mathematical Sciences, New York University

Die nachstehende Arbeit wurde im Rahmen des Vertrages zwischen dem Max-Planck-Institut für Plasmaphysik und der Europäischen Atomgemeinschaft über die Zusammenarbeit auf dem Gebiete der Plasmaphysik durchgeführt.

IPP 6/234 D.S.Harned, W.Kerner Semi-Implicit Method for Three-Dimensional Compressible MHD Simulation

Abstract

A semi-implicit method for solving the full compressible MHD equations in three dimensions is presented. The method is unconditionally stable with respect to the fast compressional modes. The time step is instead limited by the slower shear Alfven motion. The computing time required for one time step is essentially the same as for explicit methods. Linear stability limits are derived and verified by three-dimensional tests on linear waves in slab geometry.

I. Introduction

The major application of three-dimensional magnetohydrodynamic (MHD) simulation is the study of toroidal or linear plasma confinement devices, e.g. tokamaks, stellarators, reversed-field pinches, and tandem mirrors. MHD codes are extensively used for analyzing three-dimensional equilibrium configurations for stellarators and for studying the plasma evolution leading to disruptions in tokamaks. Due to the high cost of these devices and due to the structural damage caused by hard disruptions, numerical simulation plays an important role in both analysis and design studies. MHD simulation methods have been extensively reviewed by Brackbill /1/ and by Schnack and Killeen /2/.

The aforementioned devices are all characterized by a long scale length in the toroidal direction (axial for mirrors) and a much shorter scale length in the perpendicular direction. These different scale lengths lead to a separation of time scales with fast compressional waves occurring on a very rapid time scale and shear Alfven, sound, and resistive modes evolving on much slower time scales. Conventional explicit numerical schemes are forced to use very small time steps due to a Courant-Friedrichs-Lewy (CFL) condition imposed by the fast compressional modes.

One method to avoid the fast time scale restriction is to make analytic simplifications in the MHD equations by applying an expansion in the inverse aspect ratio /3,4/. These equations have been implemented numerically by a number of authors in the study of tokamak disruptions /5 - 8/. Such "reduced" equations eliminate the fast time scale; however, in order to properly include effects of finite pressure and toroidal geometry they often require retaining terms as high as third or fourth order in the expansion parameter /9,10/. Some experiments have a relatively small aspect ratio, such as JET /11/ with $R/a = 2.4$, so that inverse aspect ratio expansion does not provide a good representation.

Another approach to eliminate the fast time scale is given by the assumption of incompressibility /1,12/. While this eliminates the fast compressional modes it also has the undesirable effect of eliminating sound waves. This assumption leads to incorrect growth rates of unstable modes /13/ and for resistive instabilities it can change the stability threshold. The analysis for resistive ballooning modes reveals that compressibility stabilizes the slow resistive ballooning modes /14,15/.

In principle it is possible to eliminate the CFL restriction by using an implicit time advance. Advancing the resistive term implicitly does not pose great difficulties, but advancing the full equations implicitly in three dimensions would require the solution of very large matrix systems at every time step.

One technique to make implicit methods less cumbersome is the alternating direction implicit (ADI) method. Such a scheme has been applied to the three-dimensional MHD equations by Finan and Killeen/16/. However, this method still requires the solution of large block matrix equations in the time advance.

We conclude that it is necessary to solve the MHD equations for finite compressibility and aspect ratio without analytic approximation. The numerical scheme should be tailored to allow reasonable time steps on the shear Alfven time scale and should have the virtue of being simple to implement. For this purpose we propose here a semi-implicit method, which is aimed toward the eventual simulation of disruptions in toroidal confinement systems. Semi-implicit methods have been used previously in conventional fluid dynamics /17,18/, however their application to three-dimensional MHD is new. Our method is unconditionally stable with respect to the fast compressional modes, therefore our time step restrictions are no more severe than in the incompressible case or for the reduced equations. The method also has the virtue of not requiring the solution of any large block matrix systems in either Cartesian or cylindrical coordinates.

Only one simple tridiagonal matrix equation must be solved. The method is presented here together with a linear stability analysis. Using a three-dimensional code in slab geometry, unconditional stability with respect to the fast modes is demonstrated. Resistivity is not included in these simulations because the treatment of resistivity is independent of the method for eliminating the fast compressional time step restriction. In Section II of this paper the model is defined and the semi-implicit method for the three-dimensional MHD equations is described. In Section III we discuss the linear stability properties of the method. In Section IV the results of numerical tests are presented. Finally in Section V we present conclusions and discuss the application of the method to resistive instabilities in adapted toroidal coordinates.

II. Model

The compressible MHD equations in single fluid theory have the form:

Momentum $$\frac{\partial}{\partial t}(\rho\vec{v}) = -\nabla\cdot(\rho\vec{v}\vec{v}) + (\nabla\times\vec{B})\times\vec{B} - \nabla P \quad (1)$$

Maxwell-Ohm $$\frac{\partial\vec{B}}{\partial t} = \nabla\times(\vec{v}\times\vec{B}) - \nabla\times(\eta\,\nabla\times\vec{B}) \quad (2)$$

Continuity $$\frac{\partial\rho}{\partial t} = -\nabla\cdot(\rho\vec{v}) \quad (3)$$

Energy $$\frac{\partial P}{\partial t} = -\vec{v}\cdot\nabla P - \gamma P\nabla\cdot\vec{v} + \text{dissipative terms} \quad (4)$$

where ρ denotes the mass density, P the plasma pressure, $\vec{B}$ the magnetic field, $\vec{v}$ the flow velocity, and η the resistivity of the plasma. We are interested in problems in which wave propagation occurs most rapidly across one plane. For simplicity, Cartesian coordinates are considered here where scale lengths in the z-direction are much longer than in the x and y-directions. The fastest time scale will be due to the fast compressional waves in the x-y plane. We do not make any assumptions about aspect ratio or compressibility. In what follows we present a semi-implicit algorithm which has the advantage of having no fast time scale restriction on the time step, but solves the full MHD equations without any additional approximations.

To illustrate the semi-implicit method consider a one-dimensional linear problem with $\partial/\partial z = \partial/\partial y = 0$, $\vec{B} = B_z\hat{z}$, and $\vec{v} = v_x\hat{x}$. Assume that the plasma is cold and that the density is constant ($\rho = 1$, $P = 0$). Finally, neglect resistivity and linearize Eqs. 1 and 2 with $v_x = v_1(x)$ and $B_z = B_0 + B_1(x)$. This gives a simple set of equations which contains only fast compressional waves:

$$\frac{\partial V_1}{\partial t} = -B_0 \frac{\partial B_1}{\partial x} \tag{5}$$

$$\frac{\partial B_1}{\partial t} = -B_0 \frac{\partial V_1}{\partial x} \quad . \tag{6}$$

This set can be written easily as the second order wave equation:

$$\frac{\partial^2 V_1}{\partial t^2} = B_0^2 \frac{\partial^2 V_1}{\partial x^2} \quad . \tag{7}$$

We now consider the following discretization of Eq. 7 in time:

$$V_1^{n+1} = V_1^n + \Delta t \left(\frac{\partial V_1}{\partial t}\right)^n + B_0^2 (\Delta t)^2 \left(\frac{\partial^2 V_1}{\partial x^2}\right)^n \quad , \tag{8}$$

where $(\partial V_1 / \partial t)^n$ can be determined from Eq. 5. This is an explicit time advance and consequently leads to methods which have CFL time step restrictions on the fast modes. To make this method unconditionally stable we would like to move the term $B_0^2 (\Delta t)^2 (\partial^2 V_1 / \partial x^2)^n$ to time step n + 1, so that the method becomes implicit. In a general nonlinear problem the new field B^{n+1} is not known, so instead we subtract a similar term from each side giving a semi-implicit version of Eq. 8:

$$V_1^{n+1} - A_0^2 (\Delta t)^2 \left(\frac{\partial^2 V_1}{\partial x^2}\right)^{n+1} = V_1^n + \Delta t \left(\frac{\partial V_1}{\partial t}\right)^n + B_0^2 (\Delta t)^2 \left(\frac{\partial^2 V_1}{\partial x^2}\right)^n - A_0^2 (\Delta t)^2 \left(\frac{\partial^2 V_1}{\partial x^2}\right)^n \tag{9}$$

where A_0 is a constant. The subtraction of these new terms in Eq. 9 can have the same effect as making the fast modes implicit, even though A_0 may be very different from B_0. In fact, the method will be unconditionally stable, as for an implicit method, provided $A_0^2 > B_0^2$ (see Section III). The new terms

make the treatment of the fast compressional modes only first order accurate in time, regardless of the order of accuracy of the method prior to their inclusion. This method has similarities to semi-implicit methods used in fluid dynamics /17,18/.

We follow the same procedure in three dimensions as in the one-dimensional case. First the fast compressional modes in the x-y plane are found. For this purpose we linearize Eqs. 1 - 4, differentiate Eq. 1 with respect to time, substitute, and finally, retaining only compressional modes ($\vec{k} \perp \vec{B}$), have:

$$\frac{\partial^2(\rho_0 \vec{v}_1)}{\partial t^2} = \left(B_0^2 + \gamma p_0\right) \nabla(\nabla \cdot \vec{v}_1) \tag{10}$$

The perpendicular components of modes like those in Eq. 10 have the fastest time scale. Hence it is desirable to treat them semi-implicitly as in the 1d example. In three dimensions our method uses a predictor-corrector scheme that assumes the following form:

$$(\rho \vec{v})^* = (\rho \vec{v})^n + \theta \Delta t \, \vec{F}(\rho, \vec{v}, \vec{B}, p)^n \tag{11}$$

$$\vec{B}^* = \vec{B}^n + \theta \Delta t \, \nabla \times (\vec{v}^n \times \vec{B}^n) \tag{12}$$

$$\rho^* = \rho^n - \theta \Delta t \, \nabla \cdot (\rho \vec{v})^n \tag{13}$$

$$p^* = p^n - \theta \Delta t \, (\vec{v}^n \cdot \nabla p^n + \gamma p^n \nabla \cdot \vec{v}^n) \tag{14}$$

$$v_z^{n+1} = v_z^n + \frac{\Delta t}{\rho^*} F_z(\rho, \vec{v}, \vec{B}, p)^* \tag{15}$$

$$\vec{v}_\perp^{n+1} - \frac{(\Delta t)^2 A_0^2}{\rho^*} \nabla(\nabla \cdot \vec{v}_\perp)^{n+1} = \vec{v}_\perp^n + \frac{\Delta t}{\rho} \vec{F}_\perp(\rho, \vec{v}, \vec{B}, p)^* - \frac{(\Delta t)^2 A_0^2}{\rho^*} \nabla(\nabla \cdot \vec{v}_\perp)^n \tag{16}$$

$$\vec{B}^{n+1} = \vec{B}^{n} + \frac{\Delta t}{2} \nabla \times \left[(\vec{V}^{n+1} + \vec{V}^{n}) \times \vec{B}^{*} \right] \tag{17}$$

$$\rho^{n+1} = \rho^{n} - \frac{\Delta t}{2} \nabla \cdot \left[\rho^{*} (\vec{V}^{n+1} + \vec{V}^{n}) \right] \tag{18}$$

$$P^{n+1} = P^{n} - \frac{\Delta t}{2} \left[(\vec{V}^{n+1} + \vec{V}^{n}) \cdot \nabla P^{*} + \gamma P^{*} \nabla \cdot (\vec{V}^{n+1} + \vec{V}^{n}) \right] \tag{19}$$

$\vec{F}$, the force, is the right hand side of Eq. 1. Θ is a parameter which may be chosen to be from 0.5 to 1.0. $\vec{V}_{\perp}$ refers to the velocity in the x-y plane. A_o is again a constant which must be sufficiently large for the method to be unconditionally stable with respect to the fast modes. The magnetic field is always advanced after the velocity advance, so that it requires no special treatment. The advanced velocities may then be used in a Crank-Nicolson-type advance, as in Eq. 17. The pressure and density are also handled in this manner. If Θ is chosen to be 0.5 the method is second order accurate in time, with the exception of the fast compressional modes which remain first order accurate due to the semi-implicit terms. However, in practice we normally choose $\Theta > 0.5$ for reasons to be discussed in Sections III and IV.

Because the method is intended to eventually be used in cylindrical and adapted toroidal coordinates, we assume periodicity in y and z. In x we have conducting walls at x = 0 and x = 1. We represent quantities as a double Fourier series in y and z, i.e.

$$f = \sum_{m,n} \hat{f}_{mn}(x) \, e^{i\left(\frac{2\pi m}{a} y + \frac{2\pi n}{L} z\right)}$$

In x we use standard, centered, second order finite differences. This spatial representation leads to a large simplification in the time advance. Advancing Eqs. 11 - 19 is straightforward, except for Eq. 16. The semi-implicit term in Eq. 16 couples the V_x and V_y equations:

$$V_x^{n+1} - (\Delta t)^2 A_0^2 \left(\frac{\partial^2 V_x}{\partial x^2} + \frac{\partial^2 V_y}{\partial x \partial y} \right)^{n+1} = V_x^n + \Delta t F_x^n - (\Delta t)^2 A_0^2 \left(\frac{\partial^2 V_x}{\partial x^2} + \frac{\partial^2 V_y}{\partial x \partial y} \right)^n \tag{20}$$

$$V_y^{n+1} - (\Delta t)^2 A_0^2 \left(\frac{\partial^2 V_x}{\partial x \partial y} + \frac{\partial^2 V_y}{\partial y^2} \right)^{n+1} = V_y^n + \Delta t F_y^n - (\Delta t)^2 A_0^2 \left(\frac{\partial^2 V_x}{\partial x \partial y} + \frac{\partial^2 V_y}{\partial y^2} \right) \tag{21}$$

However, because the semi-implicit term in Eq. 21 contains no x-derivatives of V_y, after Fourier transforming, Eq. 21 can be written as:

$$\hat{V}_y^{n+1} = \hat{V}_y^n + \frac{1}{\left[1 + (\Delta t)^2 A_0^2 \left(\frac{2\pi m}{a}\right)^2\right]} \left[\Delta t \hat{F}_y^n + \left(\frac{i 2\pi m}{a}\right) A_0^2 (\Delta t)^2 \frac{\partial}{\partial x} \left(\hat{V}_x^{n+1} - \hat{V}_x^n \right) \right] \tag{22}$$

This expression is then substituted back into Eq. 20 with the result:

$$\hat{V}_x^{n+1} - (\Delta t)^2 A_0^2 \left[\frac{1}{1 + (\Delta t)^2 A_0^2 \left(\frac{2\pi m}{a}\right)^2} \right] \frac{\partial^2 \hat{V}_x^{n+1}}{\partial x^2} = \hat{V}_x^n + \frac{\left(\frac{i 2\pi m}{a}\right) (\Delta t)^3 A_0^2}{1 + (\Delta t)^2 A_0^2 \left(\frac{2\pi m}{a}\right)^2} \frac{\partial \hat{F}_y^n}{\partial x}$$

$$+ \Delta t \hat{F}_x^n - (\Delta t)^2 A_0^2 \left[\frac{1}{1 + (\Delta t)^2 A_0^2 \left(\frac{2\pi m}{a}\right)^2} \right] \frac{\partial^2 \hat{V}_x^n}{\partial x^2} \tag{23}$$

after finite differencing

This equation can be solved easily, since the left hand side is a simple tridiagonal matrix. Then the result for $\hat{V}_x^{n+1}$ is substituted back into Eq. 22 to get $\hat{V}_y^{n+1}$. Therefore, the full set, Eqs. 11 - 19, is advanced in time without requiring the solution of any large block matrix systems. We note that this also holds for cylindrical coordinates. Hence, a single time step requires essentially the same amount of computing time as an ordinary explicit advance, yet with the advantage that much larger time steps are allowed.

III. Stability

We will now demonstrate the linear stability properties of the method by analyzing a two-dimensional case with $\partial/\partial y = 0$ and $\vec{B}_o = B_{zo}\hat{z}$. With pressure set to zero and unit density, after linearization, Eqs. 11 - 19 become

$$B_{x1}^{*} = B_{x1}^{n} + \theta B_{z0} \Delta t \frac{\partial}{\partial z} V_x^n \tag{24}$$

$$B_{z1}^{*} = B_{z1}^{n} - \theta B_{z0} \Delta t \frac{\partial}{\partial x} V_x^n \tag{25}$$

$$V_x^{n+1} - (\Delta t)^2 A_o^2 \frac{\partial^2 V_x^{n+1}}{\partial x^2} = V_x^n + \Delta t B_{z0}\left(\frac{\partial B_{x1}^{*}}{\partial z} - \frac{\partial B_{z1}^{*}}{\partial x}\right) - (\Delta t)^2 A_o^2 \frac{\partial^2 V_x^n}{\partial x^2} \tag{26}$$

$$B_{x1}^{n+1} = B_{x1}^{n} + B_{z0} \frac{\Delta t}{2} \frac{\partial}{\partial z}\left(V_x^{n+1} + V_x^n\right) \tag{27}$$

$$B_{z1}^{n+1} = B_{z1}^{n} - B_{z0} \frac{\Delta t}{2} \frac{\partial}{\partial x}\left(V_x^{n+1} + V_x^n\right) \tag{28}$$

Now substitute Eqs. 24 and 25 into Eq. 26. For simplicity, here we will assume periodicity in the x-direction as well as in the z-direction. After Fourier transforming in x and z we have

$$\left(1 + A_o^2 K^2\right)\hat{V}_x^{n+1} = \left[1 + \left(A_o^2 \theta B_{z0}^2\right)K^2 \theta N^2 B_{z0}^2\right]\hat{V}_x^n + iNB_{z0}\hat{B}_{x1} - iKB_{z0}\hat{B}_{z1} \tag{29}$$

$$\hat{B}_{x1}^{n+1} = \hat{B}_{x1}^{n} + \frac{1}{2} iNB_{z0}\left(\hat{V}_x^{n+1} + \hat{V}_x^n\right) \tag{30}$$

$$\hat{B}_{z1}^{n+1} = \hat{B}_{z1}^{n} - \frac{1}{2} iKB_{z0}\left(\hat{V}_x^{n+1} + \hat{V}_x^n\right) \tag{31}$$

In Eqs. 29 - 31 N is defined as $N = (2\pi n/L)\Delta t$, where n is the mode number in the z direction. We also define K as $K = 2(\Delta t/\Delta x)\sin(k_x \Delta x/2)$. It is now suitable to write Eqs. 29 - 31 in the form $\vec{U}^{n+1} = A\vec{U}^n$, where A is the amplification matrix and $\vec{U}^T = (\hat{V}_x, \hat{B}_{x1}, \hat{B}_{z1})$. After some algebra, A is found to be

$$A = \frac{1}{Y}\begin{bmatrix} Y-\theta(K^2+N^2)B_{z0}^2 & iNB_{z0} & -iKB_{z0} \\ iNB_{z0}\left[Y-\frac{\theta}{2}(K^2+N^2)B_{z0}^2\right] & Y-\frac{1}{2}N^2B_{z0}^2 & \frac{1}{2}NKB_{z0}^2 \\ -iKB_{z0}\left[Y-\frac{\theta}{2}(K^2+N^2)B_{z0}^2\right] & \frac{1}{2}NKB_{z0}^2 & Y-\frac{1}{2}K^2B_{z0}^2 \end{bmatrix} \quad (32)$$

where $Y = 1 + A_o^2K^2$. If all eigenvalues of the matrix A are on or inside the unit circle, then no exponentially growing solutions exist and this is sufficient for numerical stability. We define the quantity α as $\alpha = (K^2 + N^2)B_o^2$. The eigenvalues of matrix A are now computed from Eq. 32, which after some algebra are eventually expressed as

$$\omega = \frac{1}{Y}\left[Y - \frac{1}{4}(1+2\theta)\alpha \pm \sqrt{-\alpha Y + \frac{1}{16}(1+2\theta)^2\alpha^2}\right] \quad (33)$$

in addition to the trivial eigenvalue, $\omega = 1$. If $\theta < 0.5$, the method is unconditionally unstable. For $0.5 \leq \theta \leq 1.0$ we have stability as long as the discriminate in Eq. 33 is not positive, i.e. whenever

$$-4(1+A_o^2K^2) + \frac{1}{4}(1+2\theta)^2(K^2+N^2)B_{z0}^2 \leq 0 \quad (34)$$

In order to have unconditional stability with respect to the fast compressional modes the method must remain stable as $K \to \infty$. From Eq. 34, it can be seen that this will be true only if the condition

$$A_o^2 > \frac{1}{16}B_{z0}^2(1+2\theta)^2 \quad (35)$$

is satisfied. Then the stability of the method will be insured with Eq. 34 by satisfying the additional condition:

$$N^2B_{z0}^2 < 16/(1+2\theta)^2 \quad (36)$$

and if Eq. 34 is satisfied

Notice first that if $\theta = 0.5$ then all roots lie on the unit circle. Therefore, even though the scheme may be stable, any excitation of the fast modes will persist as undamped noise, even for very large time steps. Additionally, if there is finite flow in the equilibrium, $\theta = 0.5$ should not be used for prediction of the advective terms, since without additional care such a method is unconditionally unstable. Therefore in practice we choose $\theta > 0.5$. If $0.5 \leq \theta \leq 1.0$, and if A_o satisfies Eq. 35, where B_{zo}^2 represents the largest value of B_z^2, then only the relatively unrestrictive condition on the shear Alfven modes, Eq. 36, must be satisfied for stability. When there is finite pressure, B_{zo}^2 is replaced by $B_{zo}^2 + \gamma P_o$ in Eq. 35.

For many problems the equilibrium field will have components in both the y and z directions (poloidal and toroidal directions in a torus). In the general case B_{zo}^2 in Eq. 35 should instead be the square of the amplitude of the total magnetic field at its maximum, rather than just the z-component. The analysis for the case with an equilibrium B_{yo} is similar to that for the case with B_{zo}. In practice, for the general three-dimensional case we find the method to be stable as long as the time step and A_o remain within the following constraints:

$$A_o^2 > \frac{1}{16}\left(B_{zo}^2 + B_{yo}^2 + \gamma P_o\right)(1+2\theta)^2 \qquad (37)$$

and

$$\left[\left(\frac{2\pi m}{a}\right) B_{yo} + \left(\frac{2\pi n}{L}\right) B_{zo}\right]^2 (\Delta t)^2 < 16/(1+2\theta)^2 \qquad (38)$$

The first constraint, Eq. 37, is the requirement for unconditional stability with respect to the fast modes and the second condition, Eq. 38, is a standard CFL-like condition imposed by the shear Alfven modes.Note that Eqs. 37 and 38 do not contain any terms involving the grid spacing in the x-direction, so that an

arbitrarily fine grid may be used in x without affecting the time step. Therefore the method satisfies our original goal of allowing reasonable time steps on the shear Alfven time scale, unrestricted by the fast compressional modes.

IV. Numerical Tests

We have tested the linear stability properties of the method in a three-dimensional code using slab geometry. We assume the density to be constant, $\rho = 1$, and neglect the advective terms. While the inclusion of these terms is necessary for a general nonlinear code, they do not affect the linear stability of the method. We initialize a uniform equilibrium magnetic field and then perturb the velocity, exciting waves. These tests have produced results consistent with the stability limits discussed in Section III.

Consider a case with $B_{zo} = 1.0$ and $B_{yo} = 0.2$. We apply the following three-dimensional perturbation, where δ is the perturbation amplitude:

$$V_x = (0.96/2\pi)\,\delta \sin(y + 0.2z) \sin(2\pi x)$$

$$V_y = 1.0\,\delta \cos(y + 0.2z) \cos(2\pi x)$$

$$V_z = -0.2\,\delta \cos(y + 0.2z) \cos(2\pi x)$$

This is an excitation of a shear Alfven wave with frequency $\omega = \vec{k} \cdot \vec{B} = 0.4$. We use 41 grid points in the x-direction. If we do not use the semi-implicit method, i.e. set $A_o = 0.0$, then numerical instability results if the time step exceeds the usual CFL condition, $\Delta t < (\Delta x / B_o) = 0.025$. In a realistic toroidal problem, including resistivity, much higher spatial resolution is required so that the CFL limit would be even more severe.

To simulate the Alfven wave we first choose a time step of $\Delta t = 0.10$, which is four times the normal CFL limit. The numerical parameter, θ, of the predictor-corrector method is set to $\theta = 0.52$ and we use $A_o = 0.7$ for the semi-implicit parameter. The kinetic energy of the wave is shown in Fig. 1. The expected wave period of $\tau = 5\pi$ is reproduced correctly. In Fig. 2 we show the result of a simulation with $\Delta t = 0.4$. Some damping of the wave kinetic energy is apparent after many oscillations, due to the predictor-corrector method. We can further increase the time step as long as it remains below the stability limit of Eq. 36. For this case the limit on the time step is $\Delta t < 4.9$. In Fig. 3 we show the wave kinetic energy as a function of time when $\Delta t = 2.0$. The wave is heavily damped. Clearly, at this point the time step is so large that the shear Alfven wave is no longer accurately represented. However, the method continues to be stable.

As a second example we consider a case with an equilibrium field purely in the z-direction, $B_{zo} = 1.0$. We set the pressure initially to $P_o = 0.3$ and $\gamma = 5/3$. Then three modes are excited: a fast compressional wave with $V_x = \delta_1 \sin(2\pi x)$, a shear Alfven wave with $V_y = \delta_2 \cos(0.2\, z)$, and a sound wave with $V_z = \delta_3 \cos(0.2\, z)$. We set $\theta = 0.52$ and $A_o = 0.8$ and again use 41 radial grid points. At first we choose a very small time step, $\Delta t = 0.01$. Figure 4 shows the kinetic energy perpendicular to B as a function of time for this case. The fast compressional wave is apparent with the proper frequency, $\omega_1 = 7.695$ ($\tau = 0.8165$). The decrease in energy is due to the beginning of a shear Alfven oscillation. We next use an increased time step of $\Delta t = 0.3$. The perpendicular kinetic energy is again shown in Fig. 5. A rapid oscillation can be seen at the beginning due to excitation of the fast compressional mode. However, the fast mode is

quickly damped, leaving only the shear Alfven wave with the proper frequency of $\omega_2 = 0.2$. In Fig. 6 the parallel kinetic energy is shown and the oscillation here is due to the sound wave with the correct frequency, $\omega_3 = \sqrt{\gamma P_o}\, k_z = 0.1414$. Figure 7 displays the time evolution of the perpendicular divergence of the velocity, $|\nabla \cdot \vec{V}_\perp|$. It shows clearly that the oscillatory compressional motion damps rapidly with large time steps. Again we emphasize that no incompressibility constraints have been enforced. The predictor-corrector method, for $\theta > 0.5$, damps any oscillatory motion when the time step is so large that this motion is not accurately resolved.

As discussed in Section III, if θ is set to $\theta = 0.50$, then any excited waves will persist undamped. We have repeated the case shown in Figs. 5 - 7 with $\theta = 0.50$. The result is shown in Fig. 8. The additional noise superposed on the shear Alfven oscillation is due to the undamped excitation of the fast modes. However, these rapid oscillations are not properly resolved with such large time steps so their excitation appears as noise. Figure 9 shows $|\nabla \cdot \vec{V}_\perp|$ for this case, indicating, in contrast with Fig. 7, that no damping of the compressional motion occurs. Therefore we again recommend keeping θ above 0.5.

Our numerical tests in three dimensions have verified our previous stability calculations. We generally find the algorithm to be numerically stable as long as the conditions of Eqs. 37 and 38 are satisfied.

V. Conclusions

We have developed a semi-implicit method for solving the full compressible MHD equations in three dimensions. The method is unconditionally stable with respect to the fast compressional modes. The time step is constrained only by the time scale of the shear Alfven modes. The method does not require the solution of any large block matrix systems; therefore, the computation time required for one time step is essentially the same as for an explicit time step. The method has been tested on linear waves in three dimensions and our stability limits have been verified.

Time steps that are much larger than fast compressional oscillation periods are permitted. However, for problems in which the dynamics of the fast modes are thought to play an important role, the details of the fast compressional motion can be fully recovered by reducing the time step.

The semi-implicit method will be applied in the future to the study of resistive instabilities in toroidal confinement devices. The addition of resistivity to our method is straightforward. The method is intended to be implemented ultimately in adapted toroidal coordinates. As is the case with the reduced equations/6/, such nonorthogonal coordinates will require more difficult matrix solutions in the velocity computation than the simple tridiagonal solutions used in Cartesian or cylindrical coordinates. Nevertheless, the semi-implicit method should make full MHD simulations as economical as previous methods for reduced or incompressible models.

Figure Captions

Fig. 1: Kinetic energy of a shear Alfven wave due to a three-dimensional perturbation, with $\omega = 0.4$ and $\Delta t = 0.1$. The semi-implicit method properly simulates the wave even though the time step is four times the usual explicit CFL limit.

Fig. 2: Kinetic energy of the wave of Fig. 1, except with $\Delta t = 0.4$.

Fig. 3: Kinetic energy of the wave of Fig. 1 with $\Delta t = 2.0$. The time step is now too large to accurately represent the shear Alfven wave. At such a large time step the wave is damped, however, the method is still stable.

Fig. 4: Plasma kinetic energy perpendicular to the equilibrium magnetic field. A fast compressional wave, a shear Alfven wave, and a sound wave have been excited. $\theta = 0.52$ and $\Delta t = 0.01$. The rapid oscillation here is due to a fast compressional wave with $\omega = 7.695$ and the slow decrease in kinetic energy is due to the beginning of a shear Alfven wave with $\omega = 0.2$.

Fig. 5: Perpendicular kinetic energy for the case of Fig. 4, but with $\Delta t = 0.3$. The rapid oscillations at the beginning are due to the fast mode and have been effectively damped after one shear Alfven period.

Fig. 6: Parallel kinetic energy for the case of Fig. 3. The oscillation is due to the sound wave with $\omega = 0.1414$.

Fig. 7: Variation of $|\nabla \cdot \vec{V}_\perp|$ as a function of time for the case of Fig. 5. The fast compressional oscillations are clearly damped on the shear Alfven time scale.

Fig. 8: Perpendicular kinetic energy for the case of Fig. 5, except with $\Theta = 0.50$. The noise superposed on the shear Alfven wave is due to the undamped fast waves which are now inaccurately resolved by the large time step.

Fig. 9: Variation of $|\nabla \cdot \vec{V}_\perp|$ for the case of Fig. 8. The compressional motion is now undamped because Θ has been reduced to $\Theta = 0.50$ from $\Theta = 0.52$ in Fig. 7.

References

/1/ J.U.Brackbill, Methods in Computational Physics (J.Killeen, Ed.), Vol. 16, p. 1, Academic Press (New York, 1976).

/2/ D.Schnack and J.Killeen, J. Comput. Phys. 35 (1980), 110.

/3/ H.R.Strauss, Phys. Fluids 19 (1976), 134.

/4/ H.R.Strauss, Phys. Fluids 20 (1977), 1354.

/5/ H.R.Hicks, B.Carreras, J.A.Holmes, D.K.Lee, and B.V. Waddell, J. Comput. Phys. 44 (1981), 46.

/6/ B.Carreras, H.R.Hicks, and D.K.Lee, Phys. Fluids 24 (1981), 66.

/7/ R.Schmalz, Comput. Phys. Comm. 30 (1983), 139.

/8/ D.Biskamp, Plasma Physics and Controlled Nuclear Fusion Research 1982, Vienna 1983, Vol. III, p. 373.

/9/ H.R.Strauss, Nucl. Fusion 23 (1983), 649.

/10/ R.Izzo, D.A.Monticello, H.R.Strauss, W.Park, J.Manickam, R.C.Grimm, and J.DeLucia, Phys. Fluids 26 (1983), 3066.

/11/ M.F.Turner, J.A.Wesson, Comput. Phys. Comm. 24 (1981), 343.

/12/ A.Y.Aydemir, and D.C.Barnes, J. Comput. Phys. 53 (1984), 100.

/13/ R.Gruber, F.Troyon, D.Berger, W.C.Bernard, S.Rousset, R.Schreiber, W.Kerner, W.Schneider, and K.V.Roberts, Comput. Phys. Comm. 21 (1981), 323.

/14/ D.Correa-Restrepo, Plasma Phys. and Contr. Nucl. Fus. Res. 1982 (Proc. 9th Int. Conf. Baltimore) Vol. II IAEA Vienna (1983), 519.

/15/ D.Correa-Restrepo, to be published.

/16/ C.H.Finan III, J.Killeen, Comput. Phys. Comm. 24 (1981), 441.

/17/ D.Gottlieb and S.A.Orszag, Numerical Analysis of Spectral Methods: Theory and Applications, Society for Industrial and Applied Mathematics (Philadelphia, 1977).

/18/ S.A.Orszag, Mon. Weather Rev., 102 (1974), 56.

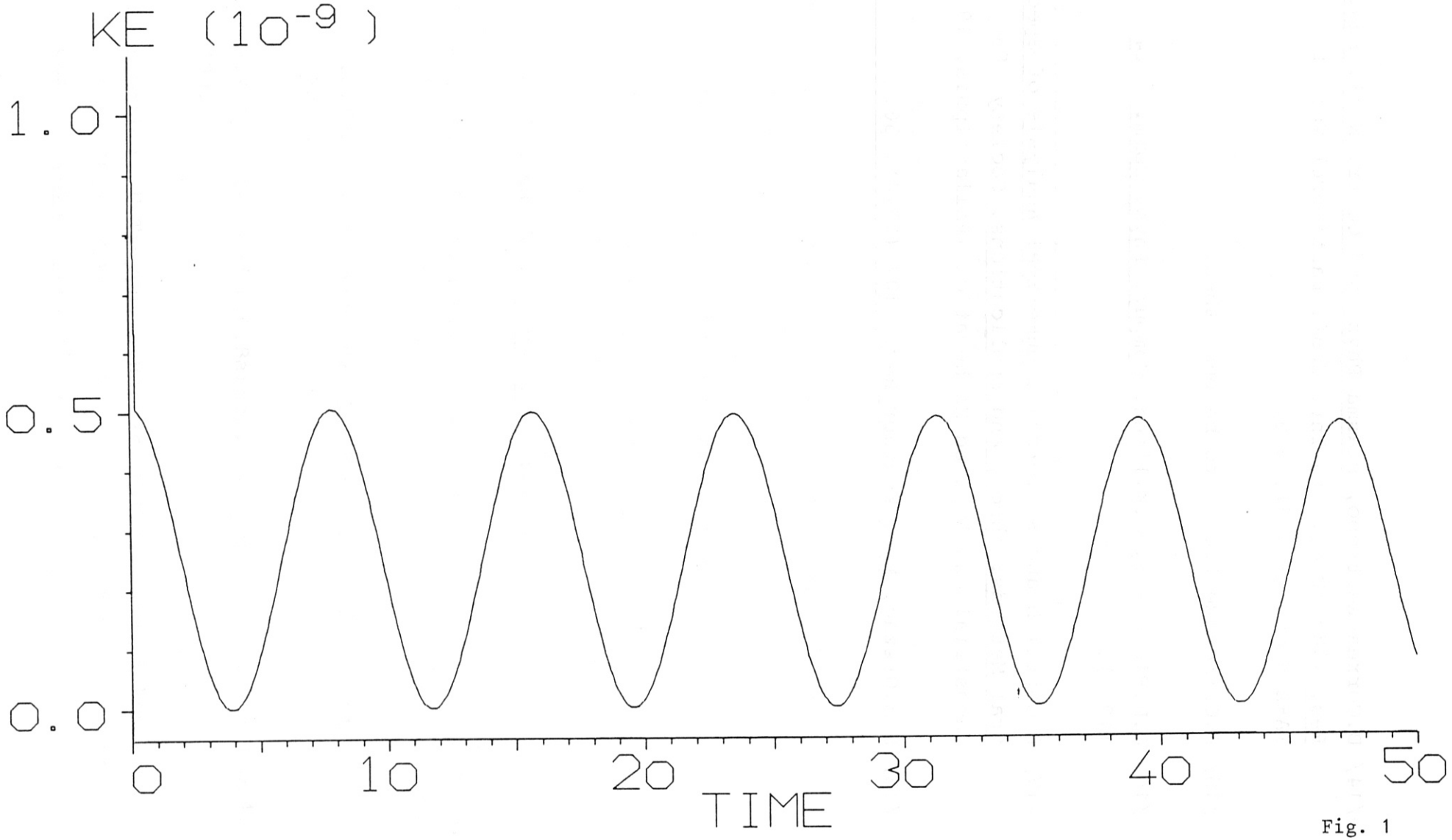

Fig. 1

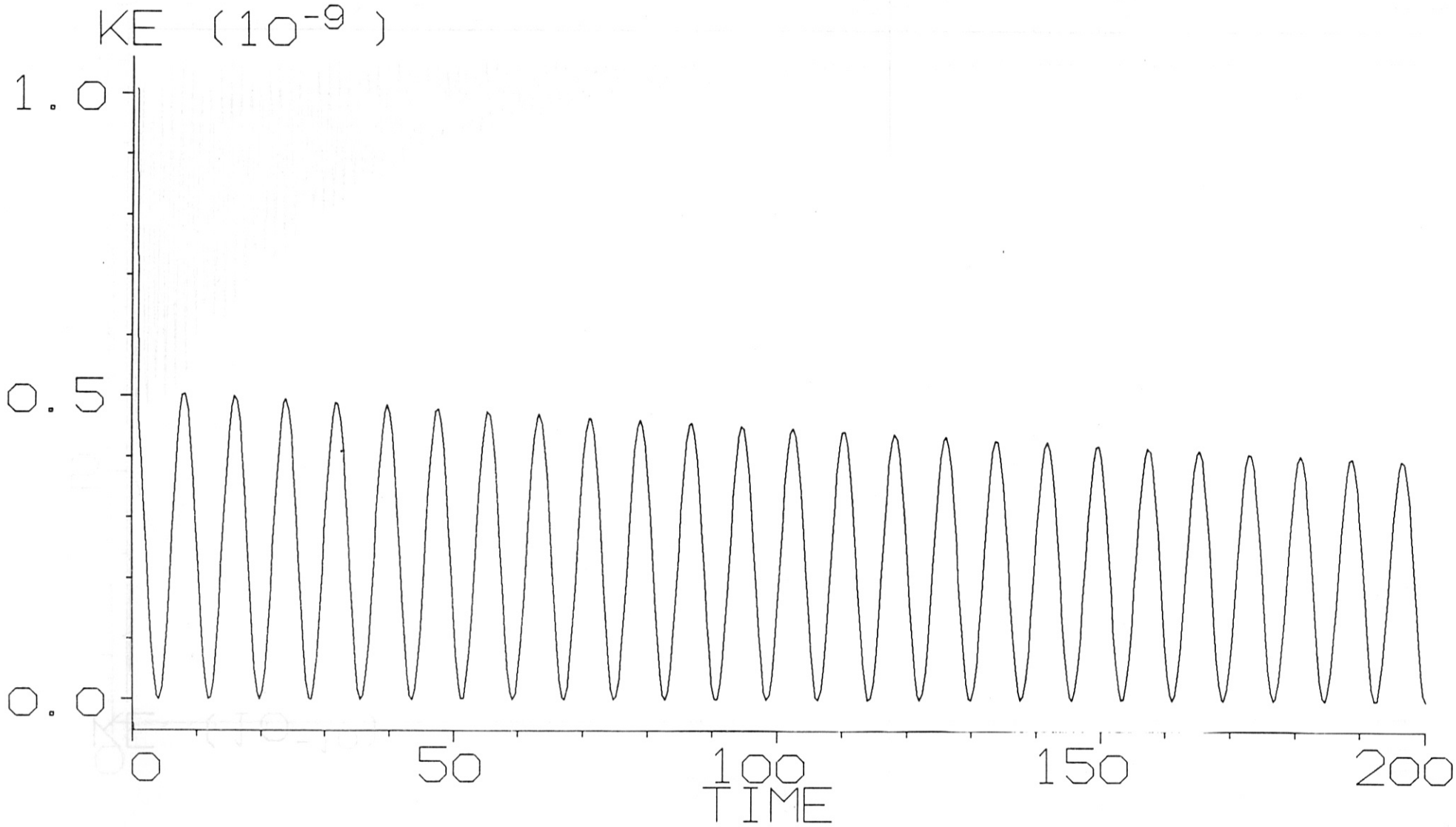

Fig. 2

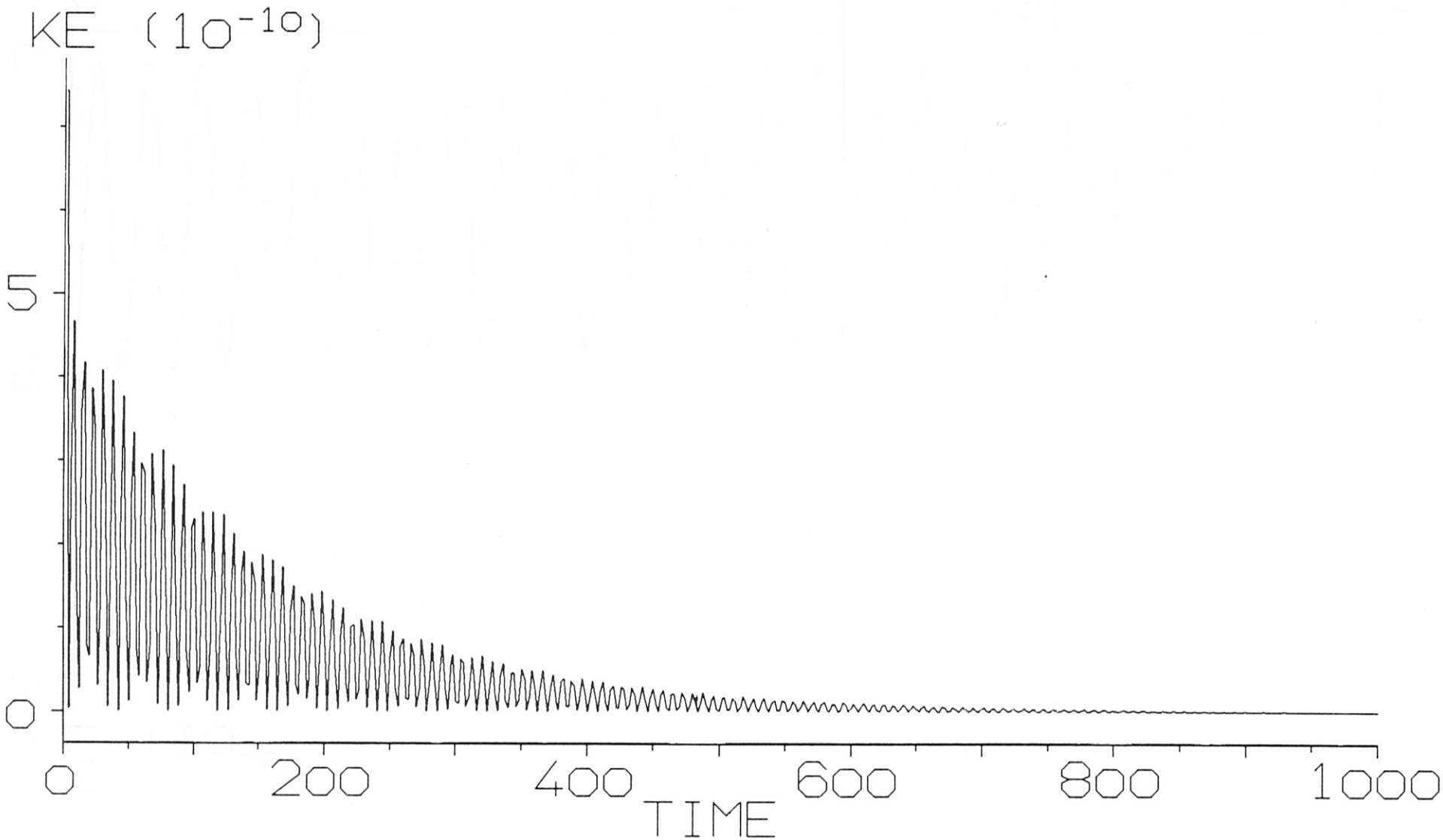

Fig. 3

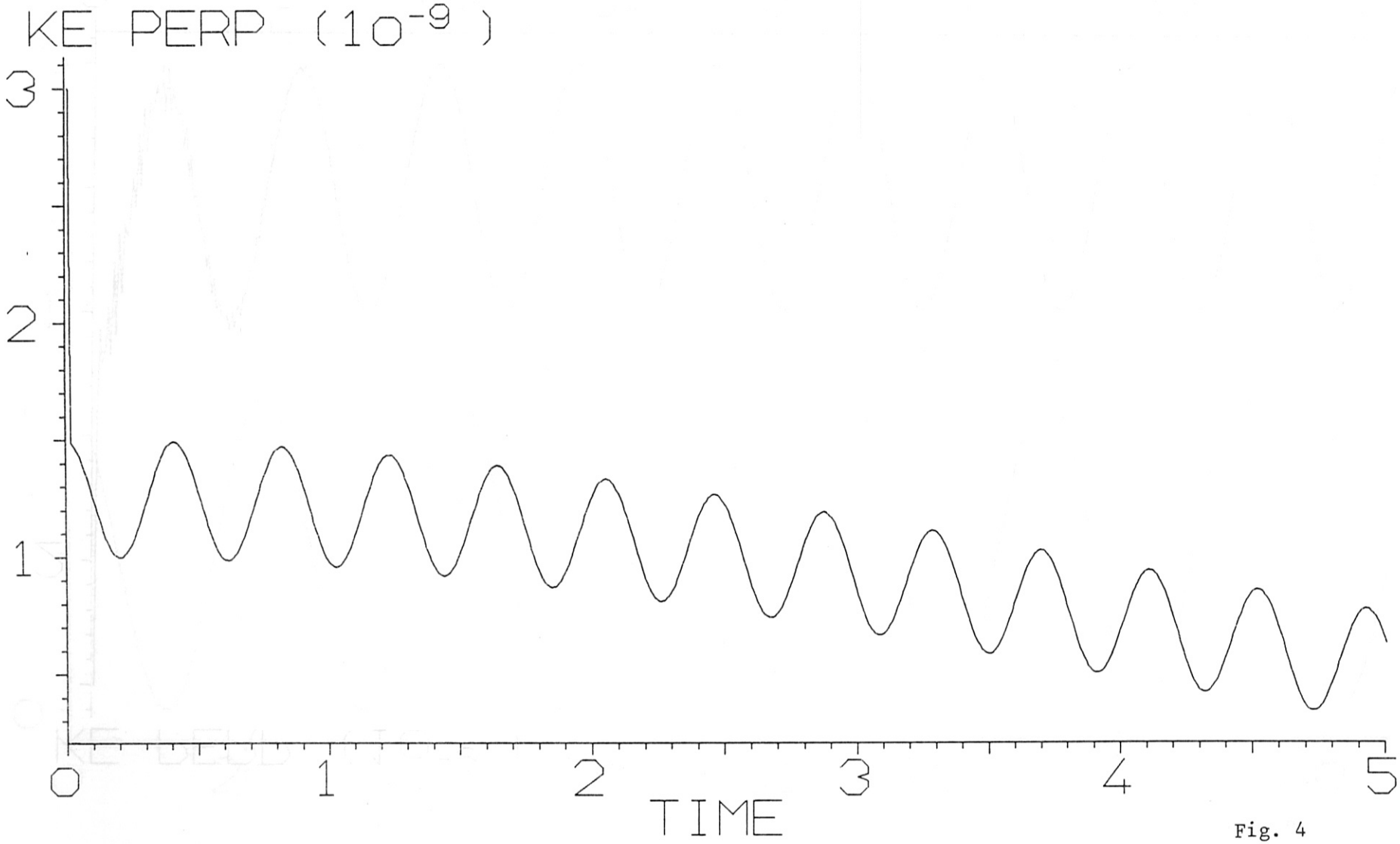

Fig. 4

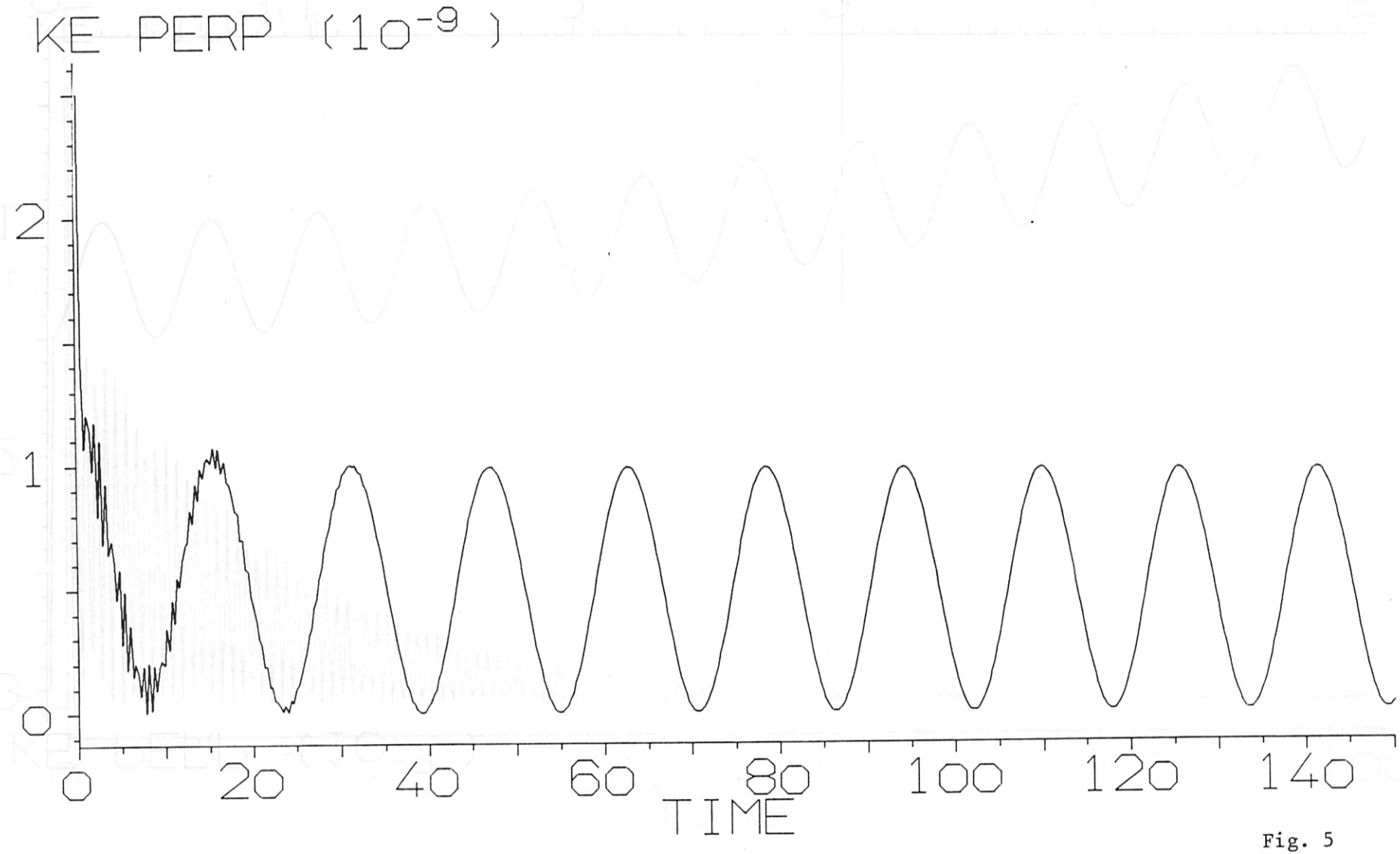

Fig. 5

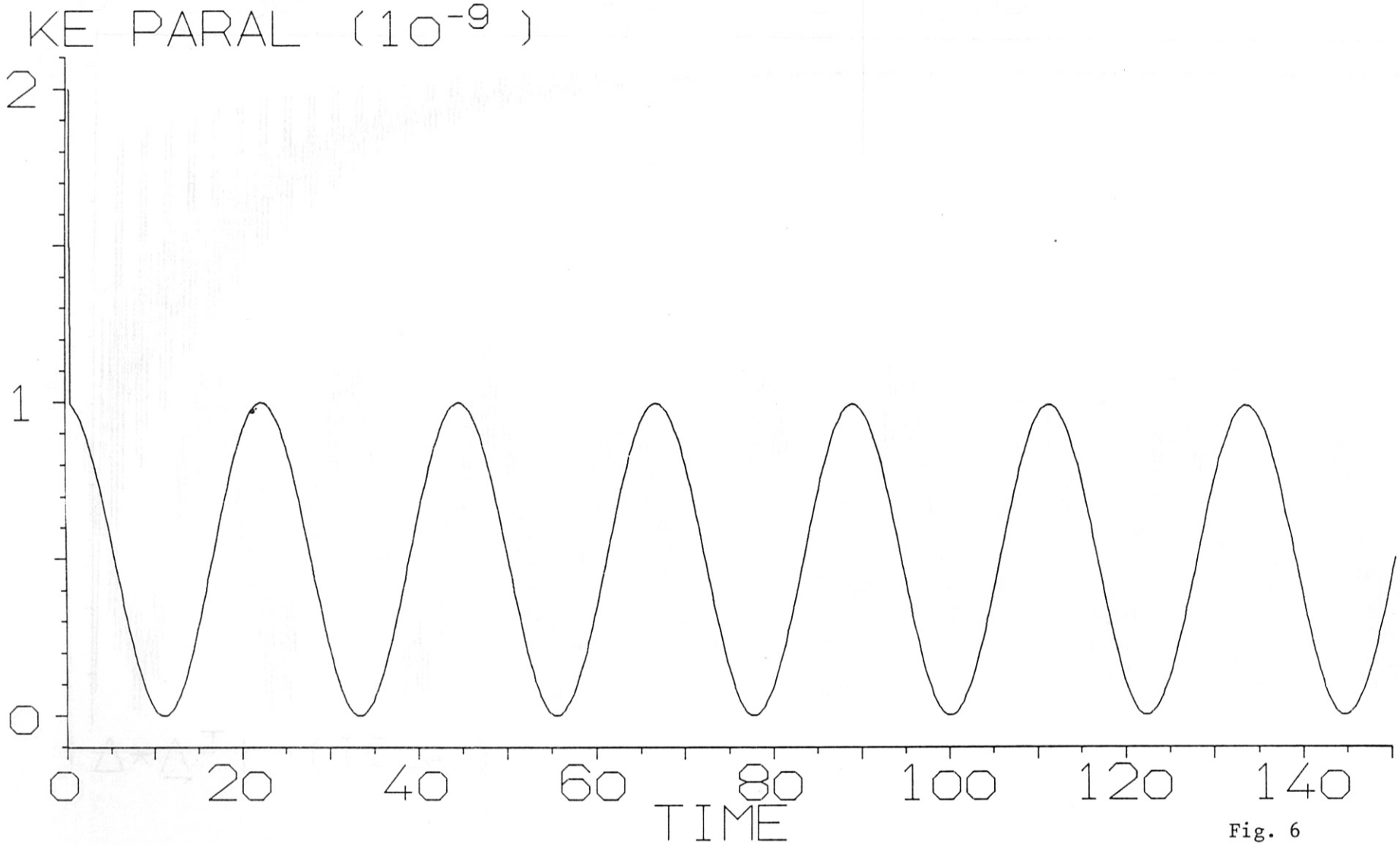

Fig. 6

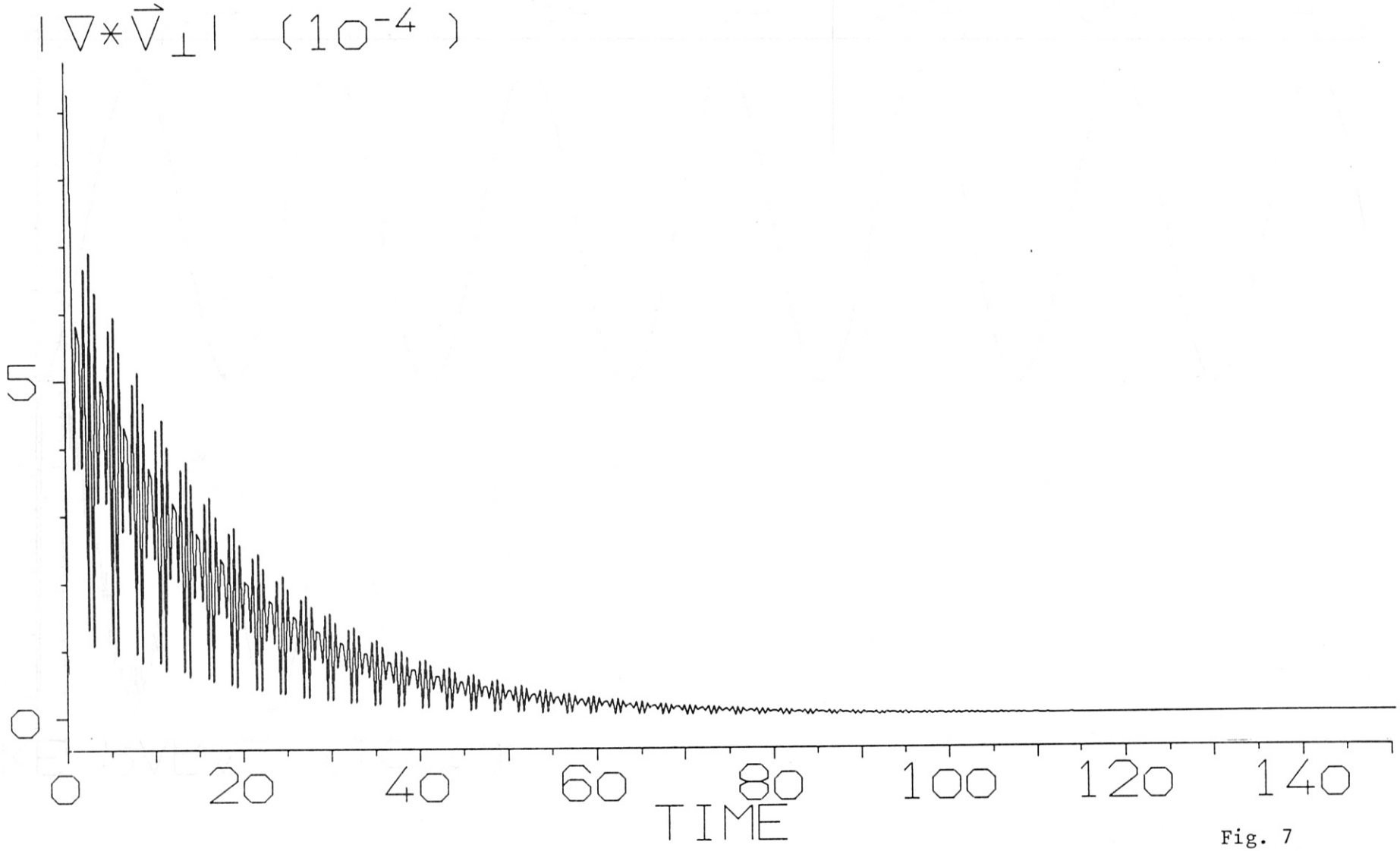

Fig. 7

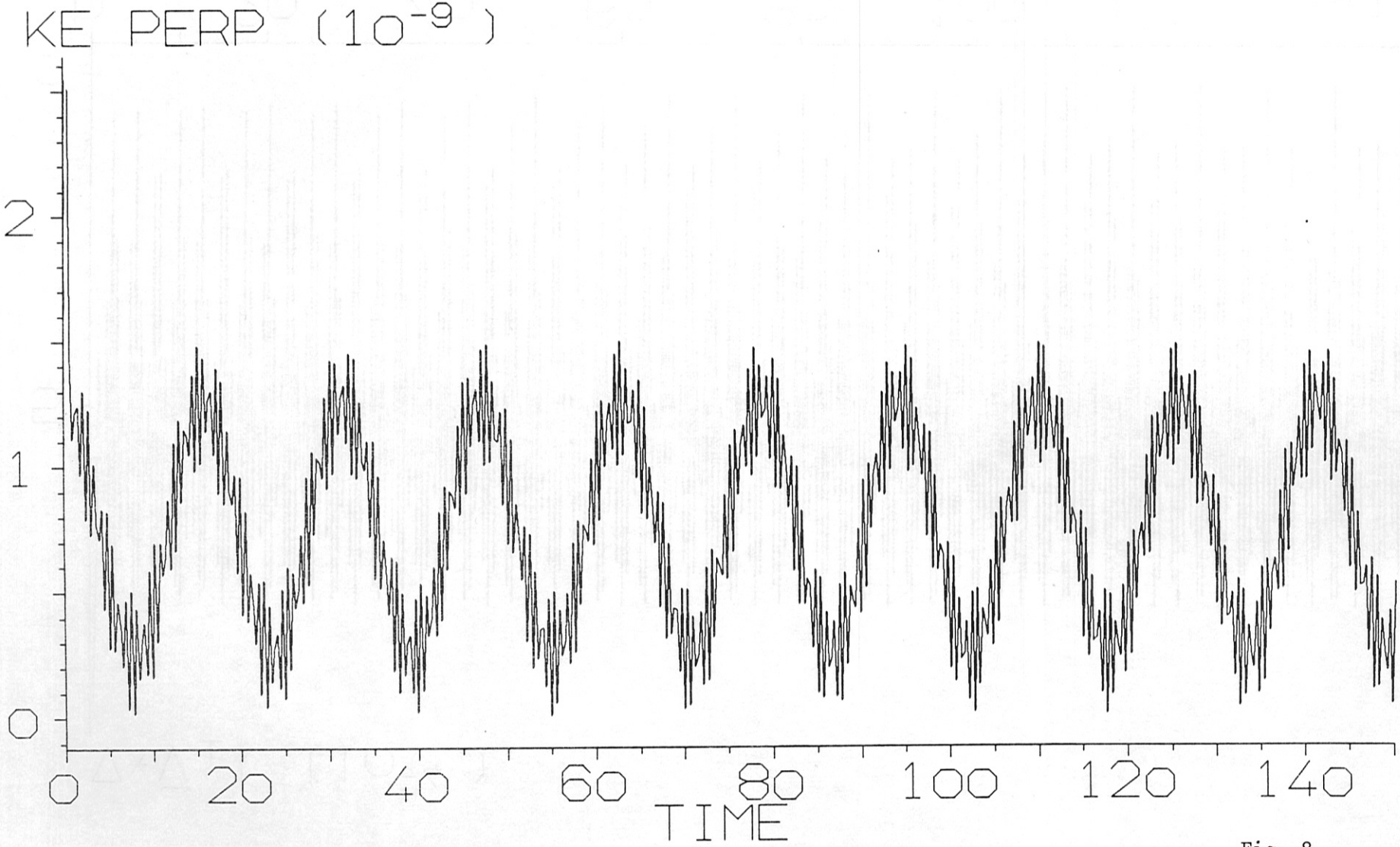

Fig. 8

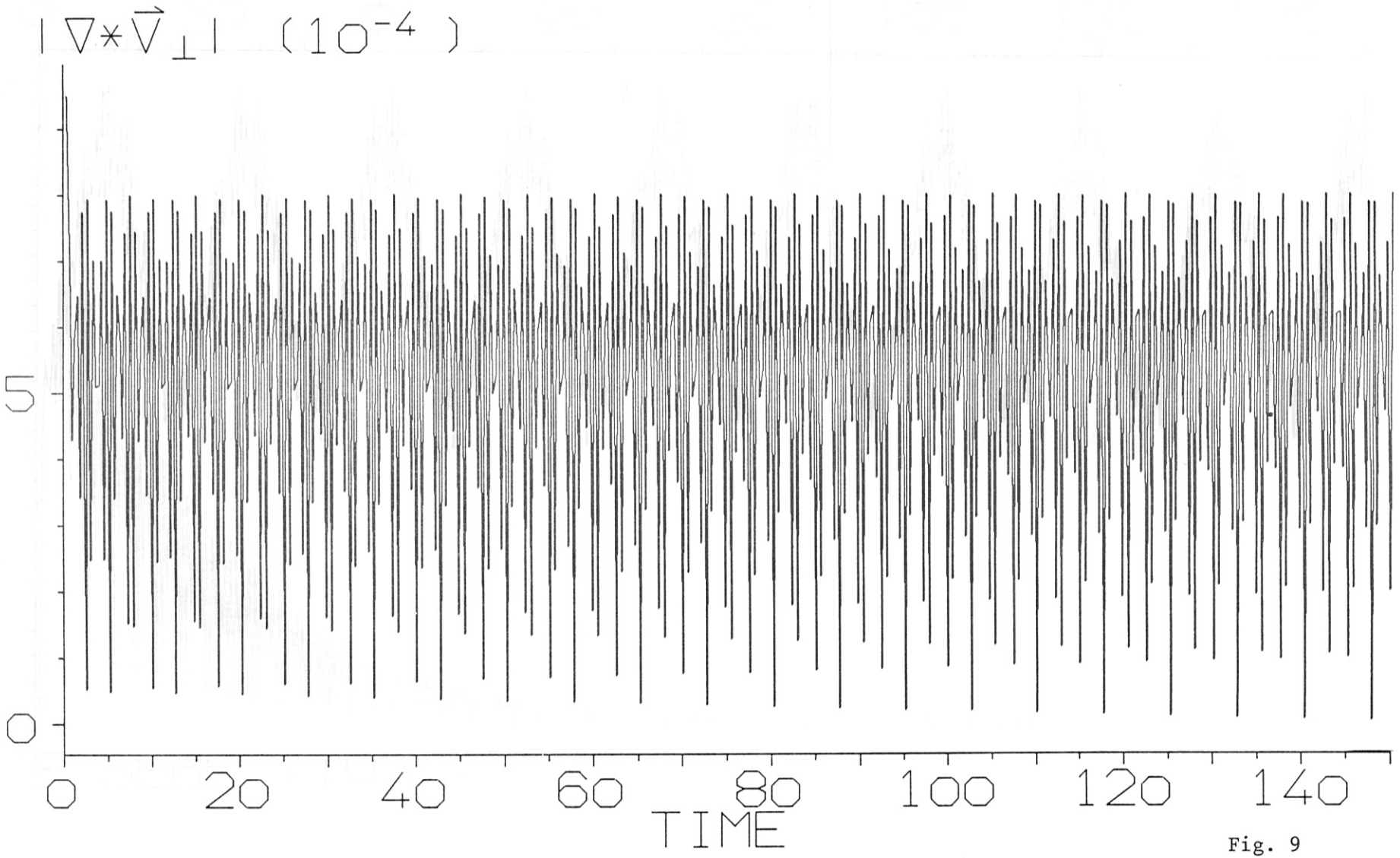

Fig. 9